Mechanisms of Development 120 (2003) 519–528

www.elsevier.com/locate/modo

Prepattern genes and signaling molecules regulate *stripe* expression to specify *Drosophila* flight muscle attachment sites

Arjumand Ghazi[1]*, Litty Paul[2], K. VijayRaghavan

National Centre for Biological Sciences, Tata Institute of Fundamental Research, GKVK PO, Bangalore 560 065, India

Received 18 November 2002; received in revised form 10 February 2003; accepted 11 March 2003

Abstract

In *Drosophila*, muscles attach to epidermal tendon cells specified by the gene *stripe (sr)*. Flight muscle attachment sites are prefigured on the wing imaginal disc by *sr* expression in discrete domains. We describe the mechanisms underlying the specification of these domains of *sr* expression. We show that the concerted activities of the *wingless* (*wg*), *decapentaplegic* (*dpp*) and *Notch* (*N*) signaling pathways, and the prepattern genes *pannier* (*pnr*) and *u-shaped* (*ush*) establish domains of *sr* expression. *N* is required for initiation of *sr* expression. *pnr* is a positive regulator of *sr*, and is inhibited by *ush* in this function. The Wg signal differentially influences the formation of different *sr* domains. These results identify the multiple regulatory elements involved in the positioning of *Drosophila* flight muscle attachment sites.

Keywords: *sr*; *wg*; *pnr*; *ush*; *dpp*; *N*; Tendon cells; Muscle attachment; Flight muscles

1. Introduction

In vertebrates, muscles attach to bones, or cartilage, with the help of tendons. Studies from the chick hind limb indicate that reciprocal muscle–tendon interactions are important for generation of the final muscle pattern (Kardon, 1998). However, the genetic, cellular and molecular mechanisms involved in this pathway remain unknown. Insect equivalents of vertebrate tendons are specialized epidermal tendon cells. Studies in *Tenebrio* (William and Caveney, 1980a,b) and *Drosophila* (Volk and VijayRaghavan, 1994) have suggested that muscle attachment sites not only supply insertion points but also provide navigational information to migrating myotubes (Frommer et al., 1996; Becker et al., 1997). In the *Drosophila* embryo, muscle attachment sites are characterized by expression of *stripe* (*sr*), a gene encoding a Zn^{++} finger protein, and a member of the vertebrate *early growth response* (*egr*) family of transcription factors. *sr* is required for specification and differentiation of tendon cells (Lee et al., 1995; Frommer et al., 1996; Fernandes et al., 1996; Nabel-Rosen et al., 1999).

The major muscles of the adult dorsal thorax are shown in Fig. 1. These muscles develop during pupation, but their attachment sites are prefigured earlier on the wing imaginal disc, in the late third instar larva, by *sr* expression at discrete positions in the presumptive notum (Fig. 1A) (Fernandes et al., 1996). *sr* expression at this stage suggests the possibility of an earlier role for the gene, in addition to its late role in tendon cell differentiation – a view strengthened by observations that flight muscles develop closely juxtaposed to *sr*-expressing attachment sites from earliest stages of adult myogenesis. Significantly, adult epidermal *sr* expression is crucial for establishing the early expression pattern of muscle founders (Dutta et al., submitted for publication). These observations, and the role of tendon cells in muscle patterning, make it important to understand the mechanisms underlying tendon cell positioning – a process dependent on the precise spatio-temporal regulation of *sr* expression. This study deciphers the mechanisms controlling *sr* expression on the wing imaginal disc.

Embryonic *sr* expression at the segment borders arises as a consequence of antagonistic interactions of *wingless (wg)*

* Corresponding author. Tel.: +1-415-476-9864; fax: +1-415-514-4145.
E-mail address: agha4664@itsa.ucsf.edu (A. Ghazi).
[1] Present address: Department of Biochemistry and Biophysics, University of California, San Francisco (UCSF), 600 16th Street, San Francisco, CA 94143-2200, USA.
[2] Present address: 484, West 12th Avenue, The Ohio State University, Columbus, OH 43210, USA.

0925-4773/03/$ - see front matter © 2003 Elsevier Science Ireland Ltd. All rights reserved.
doi:10.1016/S0925-4773(03)00042-X

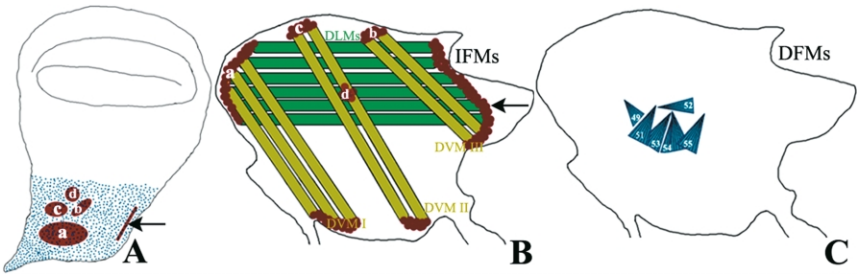

Fig. 1. Flight muscles and their attachments. (A) Schematic representation of wing imaginal disc that gives rise to a heminotum and a wing. *sr* expressing cells (red) in presumptive notum prefigure flight muscle attachment sites. Anterior attachment sites are labelled (a: medial, b–d: lateral) and arrow marks posterior DLM attachment site. Blue dots indicate myoblasts associated with presumptive notum that, during pupation, give rise to two different types of flight muscles. These muscles, from one heminotum, are shown in (B,C). (B) Indirect flight muscles (IFMs): six dorsal longitudinal muscles (DLMs, darkgreen) and three dorsoventral muscles (DVMs, light green). *sr* expressing tendon cells, to which these muscles attach (red) are labelled as in (A). IFM development has been described (Fernandes et al., 1991; Roy and VijayRaghavan, 1999). (C) Direct flight muscles (DFMs) (blue) numbered according to Miller (1950). Prominent ones shown (Ghazi et al., 2000). In all panels, anterior is to left; in B and C dorsal is to top.

and *hedgehog (hh)* signals (Piepenburg et al., 2000) and is induced by the ligands Hh, Wg and Spitz (Spi), in territories adjacent to their zones of expression (Hatini and DiNardo, 2001). However, mechanisms regulating its expression in other embryonic regions, and in the adult, are unknown. In the wing disc, *sr* expression is organized into distinct domains in the anterior and posterior compartments of the presumptive notum (Fig. 2K). This suggests that genes mediating patterning of the thoracic epidermis could act to regulate *sr*. Thoracic patterning is brought about by the concerted activities of a hierarchy of prepattern and pattern forming genes (Stern, 1954; Ghysen and Dambly-Chaudiere, 1988). The medial notum, for instance, is organized as a result of activities of the prepattern gene *pannier* (*pnr*) (Ramain et al., 1993; Heitzler et al., 1996; Calleja et al., 1996, Garcia-Garcia et al., 1999), its negative regulator *u-shaped* (*ush*) (Cubadda et al., 1997; Haenlin et al., 1997), and signaling molecules Wingless (Wg) (Phillips and Whittle, 1993) and Decapentaplegic (Dpp) (Tomoyasu et al., 1998; Tomoyasu et al., 2000; Sato and Saigo, 2000). We have studied the expression of these prepattern and pattern forming genes during adult development, to examine the extent of their overlap with different *sr* domains, and thus assign specific notal identities to the different *sr* domains. The flight muscles of hypomorphic and gain-of-function mutants of these genes have been analyzed to test for their function in thoracic myogenesis. We examine the effect of altering the expressions of these genes on the expression of *sr*. We have also examined the role of *Notch* (*N*), and its ligand *Serrate* (*Ser*) as potential regulators of *sr*. Our results indicate that *sr* activation depends on *N*, and is inhibited by *Ser*. *pnr* is crucial for initiation of *sr* expression, and its function is inhibited by *ush*. *wg*, antagonized by *dpp*, maintains the distinct identities of different *sr* domains. These results allow us to identify and describe the multiple regulatory elements involved in positioning an important class of imaginal disc derivatives – the muscle attachment sites.

2. Results

2.1. wg, pnr, ush and dpp expression domains suggest roles in sr regulation

Much of the presumptive notum is in the anterior compartment in which there are four domains of *sr* expression. One of these is in the medial region (a in Fig. 1A) and gives rise to the anterior tendon cells, to which DLMs attach (Fig. 1B). The remaining three are in the lateral region (b, c and d in Fig. 1A) and provide dorsal attachments for DVMs (Fig. 1B). In the posterior compartment, *sr* is expressed in a narrow band that eventually forms the posterior insertion site for DLMs (Fig. 1A, arrow). We examined the positioning of different *sr* domains on the wing imaginal disc, with respect to prepattern and pattern forming genes expressed in this region.

wg is expressed in a narrow region in the presumptive notum (Fig. 2B). Using a *wg lacZ* reporter, we find that *wg* expression is present between the large, medial *sr* domain and the three lateral ones (Fig. 2A–C). *wg*, at its lateral margin, borders the lateral *sr* domains and covers them partially (Fig. 2C). *pnr* expression covers the medial *sr* domain completely, whereas the lateral domains are positioned at the border of *pnr* expression (Fig. 2D–F) and the two show some overlap at the margins (Fig. 2F, white arrow). The posterior *sr* domain is also partially covered by *pnr*. The antagonist of *pnr*, *ush*, is expressed in a domain similar to *pnr* but its levels are highest at the proximal end of the disc, and gradually decrease distally. *ush* expression covers the medial *sr* domain partially (Fig. 2G-I) but does not extend to either the lateral domains or the posterior one. *sr* expression commences in regions with lowest *ush* levels, in both the proximo-distal and antero-posterior axes. This is clearest for the posterior *sr* domain, which begins at a position where *ush* expression ceases (Fig. 2I, white arrowhead). *dpp* expression is observed at the antero-posterior border of the presumptive notum in two domains, and borders *sr* expression in both the

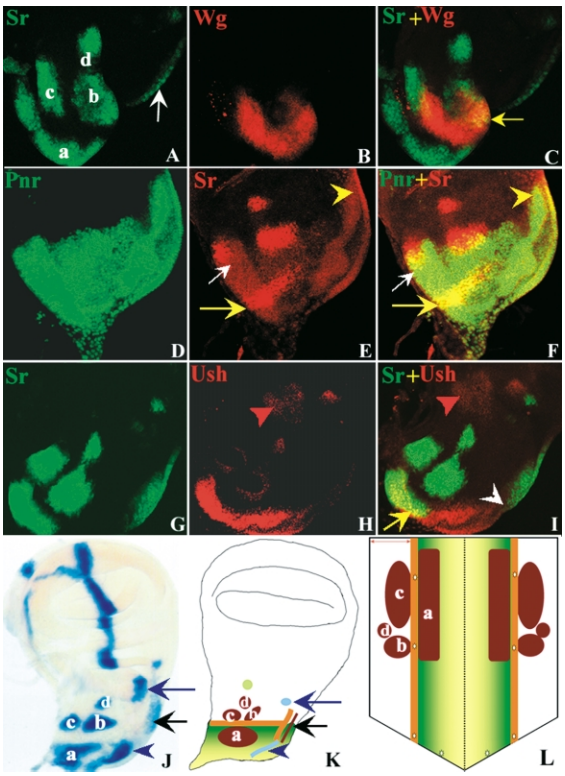

Fig. 2. Expression profiles of prepattern and pattern forming genes with respect to *sr* expressing tendon cells. (A–C): *wg* and *sr* show partially exclusive expression domains. *wg lacZ/+; srGAL4,UASGFP/+* 0 h APF prepupal wing disc labelled with anti-β-galactosidase antibody and observed for GFP fluorescence to visualize *wg* (red: B) and *sr* (green: A; anterior domains marked a–d, arrow marks posterior one). (C) Merged image. No co-localization seen except for small region near lateral domains (yellow arrow). (D–F): *pnr* completely overlaps medial *sr* domain. *pnr Gal4, P1618/UAS-nuclear GFP* 0 h APF wing disc labelled with anti-β-galactosidase antibody and observed for GFP fluorescence. (D) *pnr*-green, (E) *sr*-red, (F) merged image. Medial *sr* domain (a) lies within *pnr* region (yellow arrows in E and F); margins of two lateral domains (b and c) lie at border of *pnr* and show some overlap (white arrows in E and F). Posterior attachment site partially covered by *pnr* (yellow arrowhead in E and F). (G–I) *ush* partially overlaps medial *sr* domain: ush^{rev5}*lacZ/+; srGal4,UAS-GFP/+* 0 h APF wing disc labelled with anti-β-galactosidase antibody and observed for GFP fluorescence. (G) *sr*-green, (H) *ush*-red, (I) merged image. Co-localization (low intensity yellow, compare with F) shows *sr* expression in regions of low Ush (yellow arrow) and absent from regions of high Ush. In posterior domain, *sr* expression commences where *ush* expression ceases (white arrowhead). Second domain of *ush* near hinge, close to lateral-most *sr* domain shows reduced expression (red arrowheads). (J) *dpp* expression borders medial and lateral *sr* domains: *dppGal4-dpplacZ/+; P1618* 0 h APF wing disc labeled for β-Galactosidase activity shows both anterior medial (a) and posterior (black arrow) *sr* domains bordered by *dpp* expression (blue arrowhead and blue arrow, respectively (see the same in K). (K–L) Schematic representation of *sr*-expressing muscle attachment sites and their overlap with prepattern and pattern forming genes. *sr*-red (anterior domains labelled a–d, arrow marks posterior one), *wg*-orange, *dpp*-blue. Regions of *ush* and *pnr* co-expression shown in yellow. Gradient of yellow to green indicates progression from high to low levels of *ush* and finally only *pnr* expression, respectively. Expression profile from both imaginal discs (one shown in K) mapped onto adult dorsal notum in L (labeling as in K). In L midline indicated by stippled line and lateral notum by bi-headedarrow (top left). In all panels except L, anterior is to left. In L, view is dorsal and anterior is to top.

anterior and posterior compartments. A large domain borders the medial *sr* domain (Fig. 2J, blue arrowhead next to a) and a smaller one borders the posterior *sr* expression (Fig. 2J, blue and black arrows, respectively). The expression patterns of these genes, with respect to that of *sr*, are depicted schematically in Fig. 2K, L. This profile suggests the possibility of regulatory interactions that determine *sr* expression and these are examined below.

2.2. The Wg gradient differentially influences sr domains

To assess the extent to which different *sr* domains detect Wg, we expressed a truncated, non-functional, GPI-linked form of the Wingless receptor, DFrizzled2 (GPI-Dfz2) (Cadigan et al., 1998) in the presumptive notum. This receptor binds Wg but prevents signal transduction. Wg protein gets stabilized at the membrane and can be detected using a Wg-specific antibody. This construct has been used earlier to determine the range of *wg* signaling (Cadigan et al., 1998; Sudarsan et al., 2001). We used two different Gal4 drivers to express the *GPI-Dfz2* construct: (i) *srGal4* to express it in all the *sr* domains and examine Wg distribution within each of them and, (ii) *pnrGal4* to express in the medial notum which includes the cells transcribing *wg*. We find that not all domains of *sr* receive similar levels of Wg as

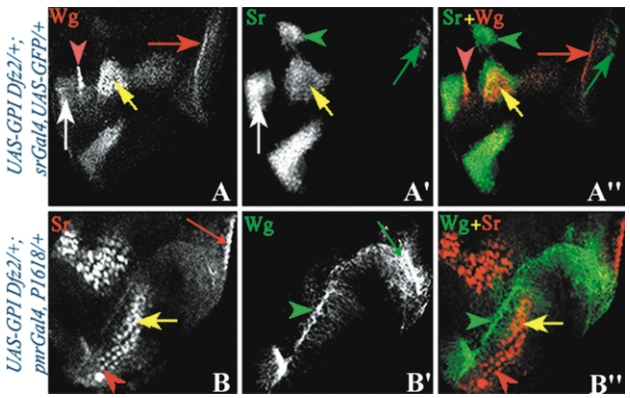

Fig. 3. The, Wg gradient differentially covers different *sr* domains. A–A″: *UAS-GPI Dfz2/+; sr Gal4, UAS-GFP/+* 0 h APF wing discs labelled with anti-Wg antibody (A, red filter) and observed for GFP fluorescence (A′, green filter). A″: Merged image. Posterior *sr* cells (green arrows in A′ and A″) receive no Wg (red arrows in A and A″); nor do cells of the lateralmost domain (d, green arrowheads in A′ and A″). Cells of domain b receive uniformly high Wg (yellow arrows, A-A″). In domain c, posterior border cells receive higher levels of Wg (red arrowheads in A, A″) than the uniform levels seen by cells in interior (white arrows in A and A′). B–B″: *UAS-GPI Dfz2/+; pnr Gal4, P1618/+* 0 h APF wing disc labelled for anti-β-Galactosidase (red filter, B) and anti-Wg (green filter, B′) antibodies. B″: Merged image. Cells in posterior *sr* domain (red arrow in B) receive no Wg (green arrow in B′; see this region in B″). In medial domain (a), cells at proximal end do not encounter Wg (red arrowhead in B, B″), whereas distal ones lie in a region which receives Wg (yellow arrows in B, B″). Cells with high levels of Wg do not express *sr* at all (green arrowheads in B′, B″, compare with same region in B). Note that co-localization does not appear yellow as Sr is nuclear and Wg is membrane bound. Code of anterior *sr* domains (a–d) same as in Fig. 2K. In all panels, anterior is to left.

seen in this assay. Cells of the posterior and most lateral (d; see Fig. 2K and IA) domains do not receive Wg at all (Fig. 3A,B″, red and green arrows). The anterior medial domain (a; see Fig. 2K and IA) lies adjacent to cells that transcribe *wg* and detects Wg protein. Cells on the lateral border of this domain receive moderate levels of Wg (Fig. 3B,B″, yellow arrows), whereas cells at the proximal end do not receive any Wg at all (Fig. 3B,B″, red arrowheads). Of the two anterior-lateral domains that lie adjacent to *wg* expressing cells (b and c; see Fig. 2K and IA), all the cells in b receive Wg, apparently uniformly (Fig. 3AA″, yellow arrows). However, cells at the posterior border of c receive high Wg signal as compared to cells in the interior of the domain (Fig. 3A,A″, red arrowheads). Thus, different domains of *sr* appear to receive different levels of Wg. We tested if different *sr* expressing cells responded differentially to changes in *wg* expression.

In animals homozygous for the *Sternopleural* (*Sp*) allele of *wg* no *wg* mRNA is detected in the presumptive notum, while wing-pouch expression remains normal (Neumann and Cohen, 1996). In *Sp* homozygotes, we find *sr* expression in a single domain (Fig. 4E; compare with wild type in B). By examining several preparations, we interpret this as the lateral domain (c) being abolished, the anterior-medial domain (a) diminished in *sr* expression and fusing with the remaining lateral domains (Fig. 4E, schematic in D). Thus, loss of *wg* expression results in loss of *sr* expression in some domains and, perhaps, a failure to establish boundaries between other domains. Mis-expression of *GPI-Dfz2*, which inactivates the *wg* signal and thus gives a partial loss of function *wg* phenotype, gives similar results. The posterior domain and most lateral domain that do not receive Wg remain unaffected (Fig. 4F, arrowhead and arrow, respectively).

Activation of *wg* signaling by misexpression of a constitutively active form of the Wg intracellular transducer, *armadillo* (*arm*), in the *pnr* domain, causes abolition of *sr* expression from most *sr* domains, except the posterior and lateral- most ones (Fig. 4C). This indicates that while some *sr* domains require *wg* for initiation of expression, high levels of Wg inhibit *sr*. These results suggest that the Wg gradient keeps the medial (a) and lateral (b, c and d) *sr* domains distinct. Conversely, we predicted that an expansion of the *wg* domain should result in domains of *sr* being more widely separated than normal. Notal *wg* expression is expanded when *scalloped* (*sd*) is misexpressed in the wing hinge region using a *vestigial (vg) GAL4* driver expressed under control of the *vg* boundary enhancer (Fig. 4H) (Varadarajan and VijayRaghavan, 1999). The mechanism underlying this is unknown but it is a useful situation to examine the effects of expanded *wg* expression on the notum (Varadarajan and VijayRaghavan, 1999). Patterning defects occur on the disc but are restricted to the wing pouch region and the presumptive notal epidermis remains normal. This can be observed in adults of the same genotype. They have disorganized wings but have nota of normal size and

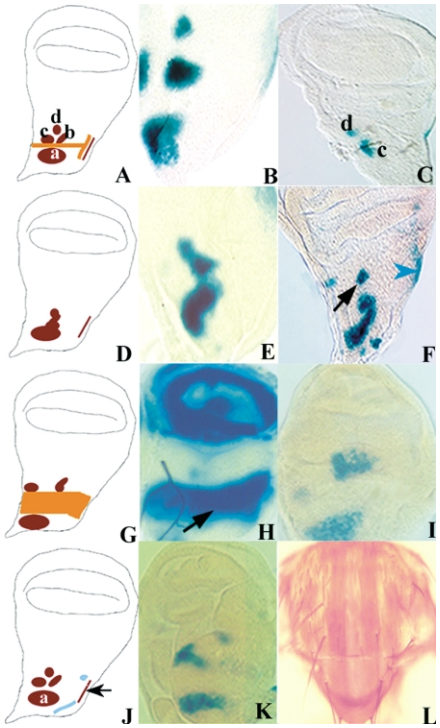

Fig. 4. *wg* and *dpp* maintain the distinct identities of *sr* domains. A, B, D–F: *sr* domains lose their distinct identities in *wg* mutants. (A) Schematic of wild type *wg* expression (orange) relative to *sr* domains (red) on wing disc. Anterior domains labelled a–d. (B) Wild type *sr* expression seen as β-Galactosidase activity in 0 h APF *Sp/CyO, MHC lacZ*; *P1618/TM3 Sb* wing disc. (D) Schematic representation of *wg* loss of function phenotype (compare with wild type schematic in A). (E) *sr* domains lose their distinction in *Sp/Sp*; *P1618/TM6 Tb* 0 h APF wing disc (compare with distinct domains in B). (F) *UAS-GPI Dfz2/+*; *pnr Gal4, P1618/+* 0 h APF wing disc. Some *sr* domains clumped into a single region. Posterior and lateral-most domains remain normal (blue arrowhead and black arrow, respectively). (G–I) Expansion of *wg* expression causes separation of *sr* domains. (G) Schematic representation of expansion of *wg* expression (compare with wild type in A). (H) Notal *wg* expression expands in 0 h APF *vgGAL4/wglacZ*; *UAS-sd/TM6 Tb* wing disc (arrow). (I) 0 h APF *vgGAL4/CyO, MHC lacZ*; *P1618/UAS-sd* wing disc, with expanded *wg* expression. Abnormally separated *sr* domains visible. (C) *pnr Gal4, P1618/UAS-activated arm* 0 h APF wing disc with *wg* activation in *pnr* domain-*sr* expression abolished in *pnr* domain but remains in domains d and c. (J–L) *dpp* maintains different *sr* domains distinct. (J) Schematic representation of *dpp* expression (blue) bordering anterior medial (a) and posterior (arrow) *sr* domains (red). (K) Reduction of *dpp* (in dpp^{d6}/dpp^{d12}; *P1618/TM6 Tb* 0 h APF wing disc) results in increased separation of *sr* domains. (L) dpp^{d6}/dpp^{d12}; *P1618/TM6 Tb* adult dorsal thorax. Normal notal morphology clear. In all panels except L, anterior is to left. In L, anterior is to top and view is dorsal.

shape (data not shown). We used this misexpression of *sd* in the wing hinge, and the consequent expansion of *wg* expression in the notum, and in this situation observed the effect on *sr* expression. The distance between the medial and lateral domains of *sr* increases (Fig. 4I, schematic in G). That these effects were not due to a general disruption of disc patterning could be discerned by observing the adults of this genotype. They showed normal notal morphology and excess dorsocentral bristles – a characteristic of increased *wg* expression in the region (data not shown). Taken

together, all these observations indicate a complex mechanism of *sr* regulation by *wg*. Moderate levels of *wg* signaling appear to be required for initiation of *sr* expression in some domains (c) but excessive *wg* signaling inhibits *sr* transcription, thus allowing the Wg gradient to keep the medial *sr* domain distinct from the lateral ones.

2.3. dpp is required to keep sr domains distinct

dpp expression along the antero-posterior border in the presumptive notum, bordering the medial *sr* domain (Fig. 4K, see Fig. 2J), is important for restricting *wg* expression in this region (Tomoyasu et al., 1998, 2000; Sato and Saigo, 2000). We investigated if *dpp* also functions in regulating *sr* expression. In dpp^{d6}/dpp^{d12}; *P1618/TM6 Tb* wing discs, *sr* domains develop much further away from each other than normal, and distance between the medial and lateral domains increases (Fig. 4K), similar to the discs with expanded *wg* expression (compare Fig. 4K with I). The normal appearance of the nota of these mutants confirmed that this effect was not due to a general disruption of notal morphology (Fig. 4L). The implications of this result – whether *dpp* acts directly on *sr*, or by regulating *wg* expression or both – are discussed later.

2.4. pnr, whose expression overlaps medial sr domain, mediates initiation of sr expression

Following the observation that *pnr* expression on the wing disc overlaps the medial *sr* domain completely, and the posterior domain partially (Fig. 5A; see Fig. 2D–F), we investigated the relationship between *pnr* and *sr* expression by examining *sr* expression in *pnr* mutants. Two classes of *pnr* allelic combinations have been described. Some, such as pnr^{md237}/pnr^{D1}, result in excess dorsocentral bristles on the notum and are categorized as 'gain of function' mutants, whereas others such as pnr^{VX1}/pnr^{V1} cause a loss of dorsocentral bristles and are categorized as 'loss of function' allelic combinations. *sr* expression in both categories was examined. A recombinant of *srGal4* with the *pnr* allele *VX1* was generated and used to follow *sr* expression. *sr* expression is reduced in its anterior domains (Fig. 5F, compare with E). The medial domain of *sr* is completely abolished, as well as parts of lateral domains that showed some overlap with *pnr*. The remaining *sr* domains are improperly positioned, presumably due to absence of *wg* mediated restriction (since *pnr* is also a regulator of *wg* expression) (Calleja et al., 1996). The posterior *sr* domain, interestingly, was expanded (Fig. 5F, arrowhead). To observe *sr* expression in the 'gain of function' mutant combination, pnr^{md237}/pnr^{D1}, a recombinant of *sr lacZ* with pnr^{md237} was generated. Surprisingly, this allelic combination also showed a complete abolition of medial *sr* domain. The possible reasons for this phenotype are discussed later. The posterior domain, however, is partially reduced in the proximal region covered by *pnr*. The lateral domains remained unaffected (Fig. 5H, compare with G).

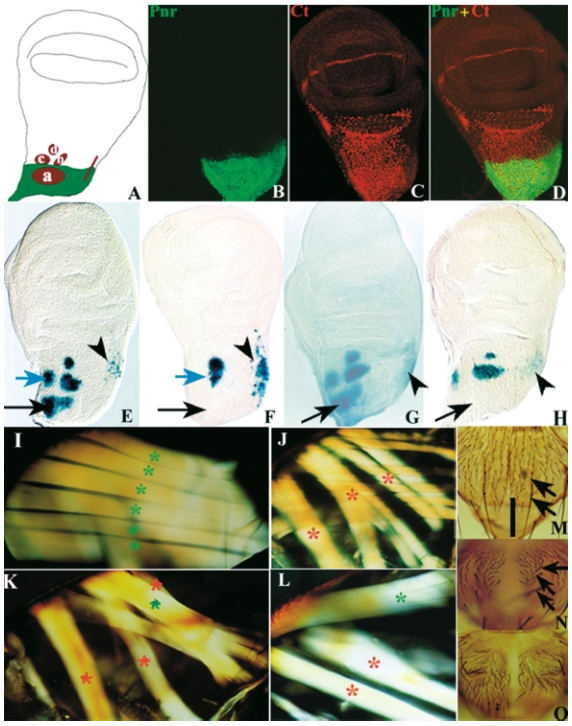

Fig. 5. *pnr* mediates initiation of *sr* expression on the wing disc. (A–D) Epidermis restricted expression of *pnr* overlaps medial *sr* domain. (A) Schematic representation of *pnr* (green) and *sr* (red) on wing disc. Anterior *sr* domains labelled a–d. (B–D) *pnrGAL4/UAS-GFP* 0 h APF wing imaginal discs labelled with anti-Cut antibodies which labels myoblasts. (B) *pnr* (green GFP). (C) Ct (red). (D) merged image. No Co-localization seen. Note that co-localization does not appear dominantly yellow in D, as the GFP is very strongly expressed in the epidermis and overwhelms the weak anti-Ct antibody. The absence of co-localization has been confirmed by confocal analysis. (E–H) Regulation of wing disc *sr* expression by *pnr*. 0 h APF wing discs labelled for *sr* expression by β-Galactosidase activity. (E) Wild type *srGal4* expression in pnr^{VX1}, *srGal4/UASnuclear lacZ*. (F) In *pnr* mutants, *UAS-nuclear lacZ/+*; pnr^{VX1}, *srGal4*/pnr^{V1}, medial *sr* domain abolished completely (compare black arrows between E and F). Of the lateral domains, only two form but are displaced and lose their distinct identities (compare blue arrows between E and F). Posterior domain slightly enlarged (compare arrowheads between E and F). (G) Wild type *sr lacZ* expression in pnr^{md237}, *P1618/TM6 Tb*. (H) In *pnr* mutant, pnr^{md237}, *P1618*/pnr^{D1}, medial *sr* domain completely, and posterior one partially abolished (compare arrows and arrowheads, respectively, between G and H). (I–L) *pnr* mutants show abnormal muscle attachments. IFMs seen under polarized light. (I) Wild type DLMs (green asterisks). (J) Wild type DVMs (red asterisks). (K) *pnr* mutants, pnr^{VX1}/pnr^{V1}- DLMs (green asterisk) reduced to a single fibre that resembles DVM III in its orientation (red asterisk at top). (L) *pnr* mutant, pnr^{md237}/pnr^{D1}-DLMs (green asterisk) appear as a single fibre. DVMs normal in both (red asterisks). Note that DVM III is not visible in this plane as it is obscured by the abnormal DLM. (M–O) Dorsal notal morphology shown in (M) wild type – note two dorsocentral bristles (arrows) and absence of notal cleft, (N) pnr^{md237}/pnr^{D1}-notal cleft associated with extra dorsocentrals (arrows) (O) pnr^{VX1}/pnr^{V1}-notal cleft associated with loss of dorsocentrals. In (A–H), anterior is to left. In (I–L), dorsal is to the top and anterior is to the left. In (M–O), anterior is to the top and the view is dorsal. Dorsal midline indicated by stippled line in M (for M–O).

We also examined flight muscles of several viable *pnr*

mutants and found DLM abnormalities (Fig. 5K,L). DLMs, which normally attach antero-posteriorly, attach abnormally and appear dorsoventral in their orientation, and resemble DVM III (Fig. 5K, compare with I and J). This suggests that attachment sites were affected in these animals due to loss of *sr* function. DVMs appear normal in all allelic combinations examined. Viable alleles of *pnr* display a mid-thoracic cleft due to failure of the two hemithoraces from fusing properly. Mutant alleles have been placed in a series depending on the severity of the cleft (Heitzler et al., 1996). To discount the possibility that muscle defects in *pnr* mutants are a consequence of this abnormality, we looked at flight muscles of mutants with different degrees of clefts. Muscle defects occur even in *pnr* allelic combinations that show no mid-thoracic cleft (data not shown). These defects must be due to *pnr* requirements on the epidermis, as the gene is not expressed in the mesoderm. No mesodermal *pnr* expression is seen at any stage. *pnrGAL4/UAS-GFP* wing discs labeled with Cut (Ct)-specific antibody – which marks adult myoblasts (Blochlinger et al., 1993) – show no colocalization of GFP with Ct-expressing myoblasts (Fig. 5B–D). The regulation of *sr* by *pnr*, the mutant phenotypes and the absence of *pnr* expression in the mesoderm suggest that the muscle defects seen are a consequence of *sr* regulation being affected.

2.5. *ush* negatively regulates *sr* expression

ush is an antagonist of *pnr* function (Cubadda et al., 1997; Haenlin et al., 1997). This information, and the observation that *sr* expression commences in regions of low *ush* expression (see Fig. 2G–I) suggested that it may be negatively regulating *sr* expression. We examined *sr* expression in *ush* mutants and misexpression contexts. In a strong viable allelic combination, ush^{VX22}/ush^{SW42}, a posterior expansion of the medial *sr* domain (a) is seen. There is also an expansion in the posterior *sr* domain (Fig. 6B, compare with A). Misexpression of *ush* in the *pnr* domain resulted in complete abolition of *sr* from all the anterior domains, except the lateralmost domain, and also from most of the posterior domain (Fig. 6C, compare with A). These results confirmed the suggestion from the expression data that *ush* exerts a negative control on *sr* expression.

We examined the flight muscles of several allelic combinations of *ush* (Cubadda et al., 1997; P. Heitzler, personal communication). Strongest defects were observed in DFMs and DLMs. DFMs, especially DFM 53, showed a striking attachment defect, in which the muscle inserts much more dorsally (arrow in Fig. 6H, compare with G). DLMs were either reduced to a single mass, or three muscles, instead of six fibres (Fig. 6E,F, compare with D).

2.6. *N* is required for initiation of *sr* expression

We also examined the role of *N* as a potential regulator of *sr*, since it is known to influence multiple events in wing

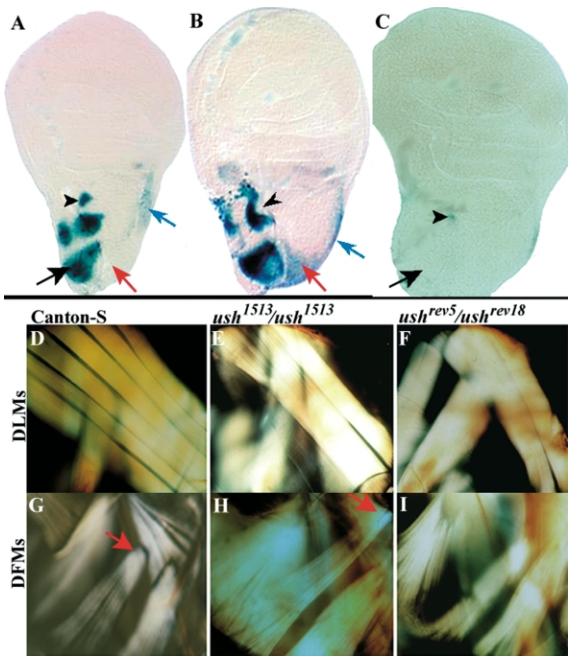

Fig. 6. *ush* inhibits *sr* expression. (A–C) *sr* is negatively regulated by *ush*. 0 h APF wing discs stained for β-Galactosidase activity. (A) *P1618*-wild type *sr*. (B) *ush* mutant, ush^{VX22}/ush^{SW42}; *P1618*/+-anterior medial *sr* domain expands posteriorly (compare red arrows between B and A), lateral domains displaced and fused abnormally (arrowhead) and posterior domain expands (compare blue arrows between B and A), C: *UAS-ush*/+; *pnrGal4/P1618*-medial and two lateral domains abolished (compare black arrows between C and A), lateral-most domain shows *sr* expression (arrowheads in C and A). (D–I): *ush* mutants show abnormal DFM attachments and DLM defects. IFMs and DFMs observed using polarized light optics. DLMs in (D) six wild type fibres (E) ush^{1513}/ush^{1513} (F) ush^{rev18}/ush^{rev5}-only two fibres in both mutants. DFMs (nomenclature in Fig. 1C) in (G) four wild type fibres (H) ush^{1513}/ush^{1513}-DFM53 attachment shifted dorsally (compare arrows between G and H) (I) ush^{rev5}/ush^{rev18}-thin and improperly attached (compare with G). In all panels, anterior is to left. In D–I dorsal is to top.

disc morphogenesis from proliferation (Go et al., 1998) to bristle patterning (Heitzler and Simpson, 1991). Using a temperature sensitive allele (N^{ts}), we inactivated the protein function by growing animals at non-permissive temperatures during the third larval instar. *sr* expression was examined at 0 h APF. Loss of *sr* expression is observed in these animals. In hemizygous males, this effect is most severe and *sr* expression is completely abolished (Fig. 7B, compare with wild type in A). Females, with one normal copy of *N*, showed faint *sr* expression (Fig. 7C, compare with wild type in A). This suggested that *N* may be required for initiation of *sr* expression. We also expressed a dominant negative form of *N* (N^{dn}), in the *pnr* domain and find abolition of *sr* expression. This was observed most clearly in the anterior medial domain covered by *pnr*. The lateral domains showed some reduction in *sr* too (Fig. 7D). In a gain of function experiment, a constitutively active form of *N* (N^{intra}) was expressed in the same region and resulted in an increase in *sr-lacZ* β-Galactosidase activity (Fig. 7E). The *N* ligand *Ser* is known to regulate *sr* expression in the

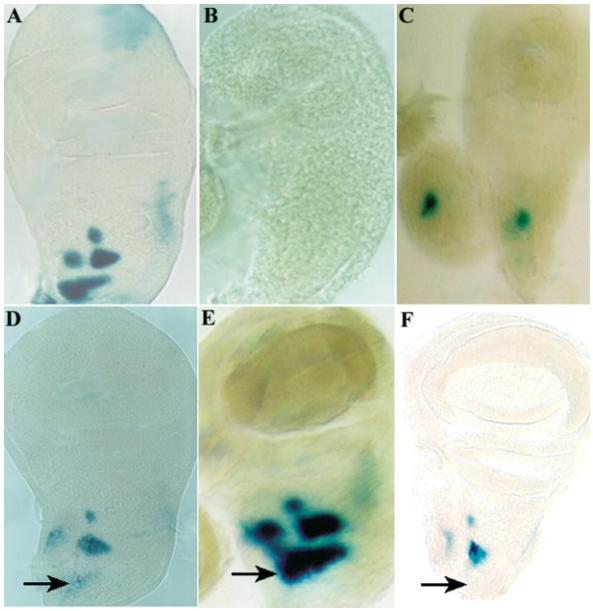

Fig. 7. *N* is required for initiation of *sr* expression. (A) Wild type *sr* expression visible as β-Galactosidase activity in *P1618* 0 h APF wing disc. (B) N^{ts}*/Y; P1618/+* 0 h APF wing disc from hemizygous male labelled for *sr* shows complete abolition of *sr* expression. The disc is also reduced in size. (C) N^{ts}*/+; P1618/+* 0 h APF wing disc from a heterozygous female with partial loss of *N* function. Some *sr* expression remains. (D) *UAS-*N^{dn}*/+; pnrGal4, P1618/+* 0 h APF wing disc grown at 29°C from mid-third instar stages labelled for *sr*. Loss of *sr* expression in the *pnr* domain (arrow) visible. There is some reduction in *sr* expression in the lateral domains too. (E) *UAS-*N^{intra}*/+; pnrGal4, P1618/+* 0 h APF wing disc grown at 29° from mid-third instar stages labelled for β-Galactosidase activity. Increased expression in the medial *sr* domain clear (arrow). There is also some increase in *sr* expression in lateral domains. (F) *UAS-Ser/+; pnrGal4, P1618/+* 0 h APF wing disc labeled for *sr* expression which is abolished from the medial domain (arrow). In all panels, anterior is to left.

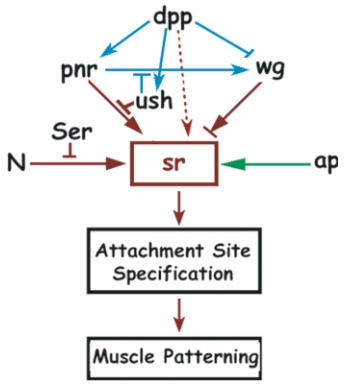

Fig. 8. Flight muscle attachment site specification occurs by concerted activities of prepattern genes and signaling pathways. Schematic representation of the genetic cascade involved in attachment site specification by regulation of *sr*. Arrows represent gene activation and bars repression. Genetic interactions identified in earlier studies (on mechanosensory bristle pattern generation) are shown in blue. Red indicates the regulatory networks revealed in this work. The prepattern gene *pnr*, expressed in an early broad domain, provides the competence for, and positively controls *sr* expression. Its negative regulator *ush* prevents this function. *N* induces *sr* and is antagonized by its ligand *Ser*. *wg* exerts a complex control on *sr* expression. At high levels, it represses *sr* transcription, whereas moderate levels are required for initiation of *sr* expression in some domains. The Wg gradient thus maintains the distinct identities of different domains. Bar and arrow between *wg* and *sr* indicate both activation and inhibition as mechanisms of regulation. *dpp* antagonizes *wg* in regulating *sr* and the stippled arrow between the genes indicate possible direct effects of *dpp* on *sr*, besides its effects through *wg, pnr* and *ush* regulation. The positive controls of *ap* on *sr* expression has been reported earlier (Ghazi et al., 2000) and is indicated by a green arrow. Data from *sr* regulation in the embryo, as well as other systems, suggests that the different regulators of *sr*, besides interacting with each other, also converge directly on enhancer(s) upstream of *sr*. (Hatini and DiNardo, 2001). A given combination of such regulatory proteins can determine precise *sr* expression in the different domains. It is also possible, as in the case of the bristle determining genes *achaete* (ac) and *scute* (sc), that individual enhancers control *sr* expression in each of its domains.

embryonic segment border cells (Hatini and DiNardo, 2001). Mis-expression of *Ser* in the presumptive notum region resulted in loss of *sr* expression (Fig. 7F). Together, these results show that the initiation of *sr* expression relies on *N*, which is antagonized by *Ser* in this activity.

3. Discussion

We have studied mechanisms underlying the specification of muscle attachment sites by control of the tendon cell marker *sr*. In this study, we show that genes that function to pattern the notal epidermis act together to specify the tendon cells to which flight muscles attach (Fig. 8).

In several developmental contexts, cell fate determination has been shown to be the result of a sequential demarcation of groups of cells (Lawrence and Struhl, 1996; Azpiazu et al., 1996). The notum is divided into checkerboard like regions of gene expression. A combination of longitudinal (*pnr* and *ush* for medial notum, *iro* locus for lateral notum) (Heitzler et al., 1996) and latitudinal (*Bar H1* and *H2* genes) (Sato et al., 1999) prepattern genes provide a framework for Wg and Dpp signaling. Regulatory networks between these genes are now being discovered and functionally mapped. In such a background, it has been instructive to map the different muscle attachment sites – as indicated by *sr* expression. Another expression profile emerges (Fig. 2K,L) that suggests regulatory interactions, between notal patterning genes and *sr* and for which we provide evidences in this study.

3.1. The complex role(s) of wg in sr regulation

The Wg gradient in the presumptive notum controls *sr* transcription differentially and keeps different *sr* domains distinct. The actual regulation of *sr* by *wg* appears to be very complex. Lateral domain c appears more sensitive to perturbations in *wg* signaling as compared to b. This is interesting since all the cells of domain b receive uniform levels of Wg whereas cells at the posterior border of c, and those bordering the posterior *sr* domain receive high Wg. One possibility is that the latter cells block progress of the Wg gradient and

thus determine responses of cells further away. This may be brought about by targeting Wg to lysosomes and degrading it, as in the embryo (Dubois et al., 2001). Another possibility, not exclusive of the first, could be that the domain and levels of *wg* transcription determine the range and gradient of Wg. The precise definition of the domain of *wg* transcription could be by mechanisms similar to that used in the wing margin (Rulifson et al., 1996). While our data suggests that the posterior and lateral-most domain do not receive Wg and may lie outside its purview, the formal possibility still exists that *wg* effects these domains in some other unknown way.

3.2. The dpp and hh pathways in sr regulation

Control of *sr* by *wg,* in segment border cells of the *Drosophila* embryo, has been demonstrated (Piepenburg et al., 2000). Wg signaling restricts *sr* activation to a single row of cells. In the presumptive notum on the wing disc, *hh* expression is restricted to a very narrow region, which forms the posterior compartment. Its effects in the disc are mediated by *dpp*, which serves multiple functions. Dpp is required for induction of *wg* expression, as it positively regulates *pnr*, which in turn activates *wg* (Tomoyasu et al., 1998; Tomoyasu et al., 2000; Sato and Saigo, 2000). However, once *wg* is induced, Dpp tightly restricts its domain. This antagonism is required for correct positioning of the DC bristles. We find that it also defines domains of *sr*. It is unclear if *dpp* directly regulates *sr*, or its effect is by control of other genes. The similarity between *sr* phenotypes observed on expansion of *wg* expression, and in *dpp* mutants, is suggestive of its effects being mediated by *wg* only, but it is also possible that it influences *sr* expression directly.

3.3. pnr, antagonized by ush, activates sr expression

Pnr, a GATA-binding protein normally functions as a transcriptional activator and is antagonized by Ush in its function. Loss of function *pnr* mutants show no *sr* expression in the domain covered by *pnr*. This, along with *sr* expansion in mutants of *ush*, would suggest that *pnr* activates *sr* in the notum, and is inhibited by *ush*. However, there is also loss of *sr* expression in *pnr* 'gain of function' mutants. The reason for this is not completely clear. One possibility is that since the mutation causes an increase in *wg* activity in the region (Calleja et al., 1996) this may cause a down-regulation of *sr*. This is supported by a similar effect seen on misexpression of activated *armadillo* in the *pnr* domain (Fig. 4C). We have taken into account results with both *pnr* and *ush* to suggest that *pnr* positively regulates *sr* and is antagonized by *ush*.

Most *sr* expression commences in regions of low *ush*. Phenotypes of *ush* mutants, and *ush* misexpression experiments, also indicate that the gene inhibits *sr*, in keeping with the simplistic scenario that *ush* antagonizes *pnr*-mediated activation of *sr*. However, the medial *sr* domain is partially covered by *ush* proximally. Further, *pnr* is known to be required for positive induction of *ush* in the embryonic epidermis (Herranz and Morata, 2001) and in some loss of function allelic combinations of *pnr*, such as pnr^{VX6}/pnr^{VX1}, there is reduced *ush* expression on the disc (Sato and Saigo, 2000). So how is *sr* initiated in the region where Pnr and Ush are co-expressed? The answer to this is not known but probably lies in levels of Ush and Pnr at that position. In loss of function *ush* mutants ectopic dorsocentral bristles form but post vertical (PV) bristles are missing (Ramain et al., 1993; Cubadda et al., 1997), suggesting that the Pnr–Ush complex acts as a repressor of the DC enhancer, but as activator of the enhancer of PV bristles. Such observations have indicated complex, context dependent interactions between Pnr and Ush in determining cell fate and could explain the regulation of *sr* expression in the medial notal region.

3.4. Domain specific regulation of sr expression

Our results indicate that each *sr* domain is regulated by a combination of prepattern genes and signaling molecules. But, a precise description of the 'combinatorial code' for regulation of each *sr* domain is beyond the scope of this work and can be achieved by generation of domain specific markers of *sr*. Based on our expression pattern data, and existing literature, we suggest that high levels of Pnr, low (or absence of) Ush and moderate levels of Wg determine the initial induction of domain a. The distinction between medial (a) and lateral (b–d) domains is established by presence of very high levels of Wg (the cells where the Wg gradient originates). Lateral expression domains are probably induced in domains controlled by the lateral prepattern gene *iro*. The differences between different lateral domains arise as a result of expression of different genes in the region. For instance, the lateral-most domain d appears to be regulated by *ush* and does not encounter Wg at all. Whereas, all cells of b receive uniformly moderate levels of Wg, only cells at the borders of c receive high Wg levels, and these differences result in the distinct identities of the two domains. Dpp, either through its effects on these regulatory genes and/or through direct effects on *sr* influences the process.

Invertebrate muscles attach to tendon cells that are entirely epidermal, unlike mesenchymal tendons of vertebrates. However, closer scrutiny of mechanisms underlying patterning of musculoskeletal system of tetrapods with those mediating insect muscle patterning suggests similarities. Some molecules involved in the two systems are conserved though the number of vertebrate players known is fewer than in *Drosophila* (Schweitzer et al., 2001). Vertebrate Tenascin (Ten), is expressed in tendons at high levels, while muscles show faint expression (Kardon, 1998). *Drosophila* Ten shows a very early and transient mesodermal expression that is replaced by distinct tendon cell

expression (Baumgartner and Chiquet-Ehrismann, 1993). In both cases, attachment tissue is marked by high Ten expression while muscles show low levels or absence. Cellular and molecular mechanisms underlying generation of vertebrate tendons are not known and in the *Drosophila* embryo the processes are only now beginning to be elucidated. Identifying genes and mechanisms that control tendon cell specification can lead to better understanding of morphogenesis and function of muscle in both vertebrates and invertebrates.

4. Materials and methods

4.1. Strains and reagents

Canton-S was used as wildtype. *pnr* alleles pnr^{D1}, pnr^{V1} and pnr^{VX1}, *UAS-pnr, ush* mutants, *UAS-ush*, *ushGal4* and *srGal4, UAS-GFP* are from Pascal Heitzler and Pat Simpson (Strasbourg, France). The following are from the Bloomington Stock Centre (Indiana, USA): pnr^{md237}, a P-Gal4 insertion allele, *wg* alleles-*en40 wg lacZ/CyO*, *dpp* alleles-*dpp Gal4, dpp lacZ/CyO-TM6 Tb,* dpp^{d6}*/CyO,* dpp^{d12}*/CyO. srlacZ (P1618)* is from Talila Volk (Weizmann Inst. Israel). *Sp/CyO, MHC lacZ; P1618/TM3 Sb* was made in this study. *UAS-GPI Dfz2* is described in Cadigan et al. (1998), and *UAS-sd* in Varadarajan and VijayRaghavan (1999).

4.2. Immunohistochemistry

β-Galactosidase (Promega) and myosin heavy chain (MHC) (Dan Kiehart, USA) specific antibodies (raised in rabbit) were used at 1:1000 and 1:500 dilutions, respectively. β-Galactosidase, Wg and Cut (Ct) specific monoclonal antibodies were used at 1:50 dilution. For fluorescent detection, Alexa568 (red) and Alexa 488 (green) secondary antibodies were used. Confocal microscopy was performed on Bio-Rad Model 1024.

4.3. Dissections

sr expression was examined in wing discs at the white prepupal stage [0 hours (h) after puparium formation (APF)]. Larvae and pupae were dissected in phosphate buffered saline (PBS), fixed in 4% paraformaldehyde and histochemically stained with X-gal (Fernandes et al., 1991) or labeled with relevant antibodies. All preparations except fluorescent samples were mounted in 70% glycerol. Fluorescent preparations were mounted in Vectashield mounting medium (Vector Chemicals). Adult hemithoraces were cut sagitally, dehydrated through 70%, 90% and 100% ethanol, cleared in methyl salicylate, mounted in Canada Balsam and observed under polarized light.

4.4. Temperature shift experiments

To examine *sr* expression in N^{ts} animals, N^{ts} virgins were crossed to *P1618 (sr lacZ)* males and progeny were grown at the permissive temperature (22°) till early late second instar to early third instar stages when they were shifted to the non-permissive temperature (31°), and grown till the 0 h APF stage for dissection.

Misexpression experiments were performed using the Gal4-UAS system described in Brand and Perrimon (1993).

Acknowledgements

We are grateful to Pat Simpson, Gines Morata, Pascal Heitzler, Helen Skaer, Dan Kiehart and Talila Volk for generous gifts of fly stocks and antibodies. The assistance of Smita Raman and M.S. Sunanda for some of the experiments is gratefully acknowledged. Our gratitude to Pat Simpson, Michael Bate, Helen Skaer and Veronica Rodrigues for stimulating discussions and many useful suggestions. Suggestions made by the anonymous reviewers helped greatly in improving the manuscript and we are thankful for this. A.G acknowledges the contribution of the late Carolyn Ann-D'Souza in generating the *CyO, MHC lacZ* balancer stock used in several experiments. This work is supported by Department of Biotechnology, India and an Indo-Israeli grant to K.V.

References

Azpiazu, N., Lawrence, P.A., Vincent, J.P., Frasch, M., 1996. Segmentation and specification of the *Drosophila* mesoderm. Genes Dev. 10, 3183–3194.

Baumgartner, S., Chiquet-Ehrismann, R., 1993. *Tena*, a *Drosophila* gene related to Tenascin, shows selective transcript localization. Mech. Dev. 40, 165–176.

Becker, S., Pasca, G., Strumpf, D., Min, L., Volk, T., 1997. Reciprocal signaling between *Drosophila* epidermal muscle attachment cells and their corresponding muscles. Development 124, 2615–2622.

Blochlinger, K., Jan, L.Y., Jan, Y.N., 1993. Postembryonic patterns of expression of *cut*, a locus regulating sensory organ identity in *Drosophila*. Development 117, 441–450.

Brand, A.H., Perrimon, N., 1993. Targeted gene expression as a means of altering cell fates and generating dominant phenotypes. Development 118, 401–415.

Cadigan, K.M., Fish, M.P., Rulifson, E.J., Nusse, R., 1998. Wingless repression of *Drosophila frizzled2* expression shapes the Wingless morphogen gradient in the wing. Cell 93 (5), 767–777.

Calleja, M., Moreno, E., Pelaz, S., Morata, G., 1996. Visualization of gene expression in living adult *Drosophila*. Science 274, 252–255.

Cubadda, Y., Heitzler, P., Ray, R.P., Bourouis, M., Ramain, P., Gelbart, W., Simpson, P., Haenlin, M., 1997. *u-shaped* encodes a zinc finger protein that regulates the proneural genes *achaete* and *scute* during the formation of bristles in *Drosophila*. Genes Dev. 11, 3083–3095.

Dubois, L., Lecourtois, M., Alexandre, C., Hirst, E., Vincent, J.P., 2001. Regulated endocytic routing modulates *wingless* signaling in *Drosophila* embryos. Cell 105 (5), 613–624.

Fernandes, J., Bate, M., VijayRaghavan, K., 1991. Development of the indirect flight muscles of *Drosophila*. Development 113, 67–77.

Fernandes, J.J., Celniker, S.E., VijayRaghavan, K., 1996. Development of the indirect flight muscle attachment sites in*Drosophila*: role of the PS integrins and the *stripe* gene. Dev. Biol. 176, 166–184.

Frommer, G., Vorbruggen, G., Pasca, G., Jackle, H., Volk, T., 1996. Epidermal *egr*-like zinc finger protein of *Drosophila* participates in myotube guidance. EMBO J. 15, 1642–1649.

Garcia-Garcia, M.J., Ramain, P., Simpson, P., Modolell, J., 1999. Different contributions of *pannier* and *wingless* to the patterning of the dorsal mesothorax of *Drosophila*. Development 126, 3523–3532.

Ghazi, A., Anant, S., VijayRaghavan, K., 2000. *apterous* mediates development of direct flight muscles autonomously and indirect flight muscles through epidermal cues. Development 127, 5309–5318.

Ghysen, A., Dambly-Chaudiere, C., 1988. From DNA to form: the *achaete-scute* complex. Genes Dev. 2, 495–501.

Go, M.J., Eastman, D.S., Artavanis-Tsakonas, S., 1998. Cell proliferation control by *Notch* signaling in *Drosophila* development. Development 125 (11), 2031–3040.

Haenlin, M., Cubadda, Y., Blondeau, F., Heitzler, P., Lutz, Y., Simpson, P., Ramain, P., 1997. Transcriptional activity of *pannier* is regulated negatively by heterodimerization of the GATA DNA-binding domain with a cofactor encoded by *the u-shaped* gene of *Drosophila*. Genes Dev. 11, 3096–3108.

Hatini, V., DiNardo, S., 2001. Distinct signals generate repeating striped pattern in the embryonic parasegment. Mol. Cell 7 (1), 151–160.

Heitzler, P., Simpson, P., 1991. The choice of cell fate in the epidermis of *Drosophila*. Cell 64 (6), 1083–1092.

Heitzler, P., Haenlin, M., Ramain, P., Calleja, M., Simpson, P., 1996. A genetic analysis of *pannier*, a gene necessary for viability of dorsal tissues and bristle positioning in *Drosophila*. Genetics 143, 1271–1286.

Herranz, H., Morata, G., 2001. The functions of pannier during *Drosophila* embryogenesis. Development 128 (23), 4837–4846.

Kardon, G., 1998. Muscle and tendon morphogenesis in the avian hind limb. Development 125, 4019–4032.

Lawrence, P.A., Struhl, G., 1996. Morphogens, compartments, and pattern: lessons from *Drosophila*? Cell 85, 951–961.

Lee, J.C., VijayRaghavan, K., Celniker, S.E., Tanouye, M.A., 1995. Identification of a *Drosophila* muscle development gene with structural homology to mammalian early growth response transcription factors. Proc. Natl Acad. Sci. USA 92, 10344–10348.

Miller, A., 1950. The internal anatomy and histology of the imago of *Drosophila melanogaster*. In: Demerec, M., (Ed.), The Biology of Drosophila, pp. 420–534.

Nabel-Rosen, H., Dorevitch, N., Reuveny, A., Volk, T., 1999. The balance between two isoforms of the *Drosophila* RNA-binding protein how controls tendon cell differentiation. Mol. Cell 4, 573–584.

Neumann, C.J., Cohen, S.M., 1996. *Sternopleural* is a regulatory mutation of *wingless* with both dominant and recessive effects on larval development of *Drosophila melanogaster*. Genetics 142, 1147–1155.

Phillips, R.G., Whittle, J.R., 1993. *wingless* expression mediates determination of peripheral nervous system elements in late stages of *Drosophila* wing disc development. Development 118, 427–438.

Piepenburg, O., Vorbruggen, G., Jackle, H., 2000. *Drosophila* segment borders result from unilateral repression of *hedgehog* activity by *wingless* signalling. Mol. Cell 6, 203–209.

Ramain, P., Heitzler, P., Haenlin, M., Simpson, P., 1993. *pannier*, a negative regulator of *achaete* and *scute* in *Drosophila*, encodes a zinc finger protein with homology to the vertebrate transcription factor GATA-1. Development 119, 1277–1291.

Roy, S., VijayRaghavan, K., 1999. Muscle pattern diversification in *Drosophila*: the story of imaginal myogenesis. Bioessays 21, 486–498.

Rulifson, E.J., Micchelli, C.A., Axelrod, J.D., Perrimon, N., Blair, S.S., 1996. *wingless* refines its own expression domain on the *Drosophila* wing margin. Nature 384 (6604), 72–74.

Sato, M., Kojima, T., Michiue, T., Saigo, K., 1999. *Bar* homeobox genes are latitudinal prepattern genes in the developing *Drosophila* notum whose expression is regulated by the concerted functions of *decapentaplegic* and *wingless*. Development 126, 1457–1466.

Sato, M., Saigo, K., 2000. Involvement of *pannier* and *u-shaped* in regulation of *decapentaplegic* dependent *wingless* expression in developing *Drosophila* notum. Mech. Dev. 93, 127–138.

Schweitzer, R., Chyung, J.H., Murtaugh, L.C., Brent, A.E., Rosen, V., Olson, E.N., Lassar, A., Tabin, C.J., 2001. Analysis of the tendon cell fate using Scleraxis, a specific marker for tendons and ligaments. Development 128 (19), 3855–3866.

Stern, C., 1954. Two or three bristles. Am. Sci. 42, 213–247.

Sudarsan, V., Anant, S., Guptan, P., VijayRaghavan, K., Skaer, H., 2001. Myoblast diversification and ectodermal signaling in *Drosophila*. Dev. Cell 1 (6), 829–839.

Tomoyasu, Y., Nakamura, M., Ueno, N., 1998. Role of *dpp* signalling in prepattern formation of the dorsocentral mechanosensory organ in *Drosophila melanogaster*. Development 125, 4215–4224.

Tomoyasu, Y., Ueno, N., Nakamura, M., 2000. The Decapentaplegic morphogen gradient regulates the notal *wingless* expression through induction of *pannier and u-shaped* in *Drosophila*. Mech. Dev. 96, 37–49.

Varadarajan, S., VijayRaghavan, K., 1999. *scalloped* functions in a regulatory loop with *vestigial* and *wingless* to pattern the *Drosophila* wing. Dev. Genes Evol. 209, 10–17.

Volk, T., VijayRaghavan, K., 1994. A central role for epidermal segment border cells in the induction of muscle patterning in the *Drosophila* embryo. Development 120, 59–70.

Williams, G.J., Caveney, S., 1980a. A gradient of morphogenetic information involved in muscle patterning. J. Embryol. Exp. Morphol. 58, 35–61.

Williams, G.J., Caveney, S., 1980b. Changing muscle patterns in a segmental epidermal field. J. Embryol. Exp. Morphol. 58, 13–33.